Photochemical Reaction Dynamics of the $N_2O{\cdot}H_2{}^{18}O$ van der Waals Complex

Nobuaki Tanaka, Umpei Nagashima,† Masao Takayanagi,‡ Hong Lae Kim,§ and Ichiro Hanazaki*

Institute for Molecular Science, Myodaiji, Okazaki 444, Japan

Received: June 27, 1996[⊗]

The rotational and vibrational energy distributions have been determined for the OH radicals resulting from the 193 nm photolysis of the van der Waals complex $N_2O{\cdot}H_2O$. Laser-induced fluorescence was used to probe the OH radicals. The rotational distributions of OH are characterized by the Boltzmann temperatures of 1700 K for ^{16}OH $v'' = 0$ and $v'' = 1$ and of 1600 K for ^{18}OH $v'' = 0$. A quantity of 29% ^{16}OH exists in the $v = 1$ state, while ^{18}OH is produced almost exclusively in the $v = 0$ state. A possible reaction scheme is discussed based on the comparison of the present results with the corresponding bimolecular reaction and with the O_3/H_2O system.

I. Introduction

Photochemistry of van der Waals complexes provides us with an opportunity to study the effect of weak intermolecular bonding on reaction dynamics. Since successful applications of this idea to the "half reaction",[1−3] many attempts have been made to elucidate the reaction mechanism and potential surfaces involved.[4] Studies of these complexes had been expected to reveal the effects of restriction of the orientation of attacking and of the impact parameter on the reaction cross section. However, after some progress of the research in this field, it was found that the effect of complex formation is not as simple as expected initially. For example, the complex formation sometimes brings about a complete switching of the reaction mechanism to another rather than the simple restriction of the attacking mode in the corresponding bimolecular reaction.

The hydroxyl radical is one of the simplest and well-characterized molecule suitable for the spectroscopic investigation. It is also known to play a central role as a reaction intermediate in atmospheric chemistry. Among several reactions producing the OH radical, the reaction of water with the oxygen atom in the ^1D state, $O(^1D) + H_2O \rightarrow 2OH(^2\Pi)$, has been studied extensively.[5−13] An advantage of studying this system is that we can distinguish OH produced by the abstraction of H by $O(^1D)$ and OH left after the abstraction by using isotopically substituted water, $H_2{}^{18}O$.[7−13] In the case of bimolecular reactions, the newly formed ^{16}OH has been found to be vibrationally and rotationally more excited than ^{18}OH, which is left after the abstraction.[13] This suggests that the reaction proceeds through the direct H abstraction mechanism or through a short-lived intermediate so that no sufficient time is available for the internal energy to be randomized during the reaction. The rotational excitation in ^{16}OH occurs through the torque imparted by the movement of attacking ^{16}O, while ^{18}OH is weakly excited by a torque imparted on the exit surface after the reaction barrier.

Recently, King and co-workers have studied the reactant-pair reaction, $O_3{\cdot}H_2{}^{18}O + h\nu \rightarrow {}^{16}OH + {}^{18}OH + O_2$, to see how the molecular environment in the van der Waals complex would affect the rotational, vibrational, and translational energy distributions in the products.[14] They found that the internal excitation is much lower for the reactant-pair reaction than that for the corresponding bimolecular reaction.

We have reported a preliminary result for the $N_2O{\cdot}H_2O$ complex using normal H_2O, where much colder rotational distributions of OH were observed than those in the corresponding bimolecular reaction.[15] In this paper, we present the results of measurements on the vibrational and rotational state distributions for OH produced in the reactant-pair reaction,

$$N_2{}^{16}O{\cdot}H_2{}^{18}O + h\nu\ (193\ \text{nm}) \rightarrow N_2 + {}^{16}OH + {}^{18}OH \qquad (1)$$

under a supersonic free jet condition to examine the effect of complex formation and to compare the results with the photolysis of $O_3{\cdot}H_2O$, for which the excess energy and the structure of the complex are different from $N_2O{\cdot}H_2O$. The use of N_2O as a precursor of $O(^1D)$ is also advantageous over O_3, since the former produces $O(^1D)$ almost exclusively[16] while the 266 nm photolysis of O_3 produces ca. 10% of $O(^3P)$ in addition to $O(^1D)$.[17]

II. Experimental Section

An excimer laser (MPB Technologies, PSX-100 or Lambda Physik, COMPex 200) was operated at 193 nm (ArF, 4 mJ/pulse, 3 ns or 50 mJ/pulse, 15 ns, 10 Hz repetition rate) to photolyze N_2O. The product OH was probed by the laser-induced fluorescence (LIF) technique applied to the OH A−X transition with a frequency-doubled dye laser (Lambda Physik, FL3002, sulforhodamine 620 or rhodamine 640) pumped by a XeCl excimer laser (Lumonics, HE-420-SM-B). Typically, the probe laser was fired with a 200 ns delay after the ArF laser irradiation. The former was operated at lower power levels (∼3 μJ/pulse) to prevent the saturation of transitions. The photolysis and probe laser beams counterpropagated in the chamber and interacted with the supersonic beam at a point 20 mm downstream from the nozzle. The laser beam diameters were typically 2 mm in the interaction region. Fluorescence was collected at a right angle to the laser beams by a photomultiplier tube (Hamamatsu, R943-02) using a gated photon counter (SRS, SR400) through a cutoff filter (Hoya, UV-28) and a band-pass filter (Hoya, U-340). The LIF signals were corrected for fluctuations in the photolysis and probe laser intensities, which

† Present address: Department of Information Science, Ochanomizu University, 2-1-1 Otsuka, Bunkyo, Tokyo 112, Japan.

‡ Present address: Graduate School of BASE (Bio-Applications and Systems Engineering), Tokyo University of Agriculture and Technology, 3-5-8 Saiwaicho, Fuchu, Tokyo 183, Japan.

§ Present address: Department of Chemistry, Kangweon National University, Chuncheon 200−701, Korea.

⊗ Abstract published in *Advance ACS Abstracts,* January 1, 1997.

S1089-5639(96)01909-3 CCC: $14.00

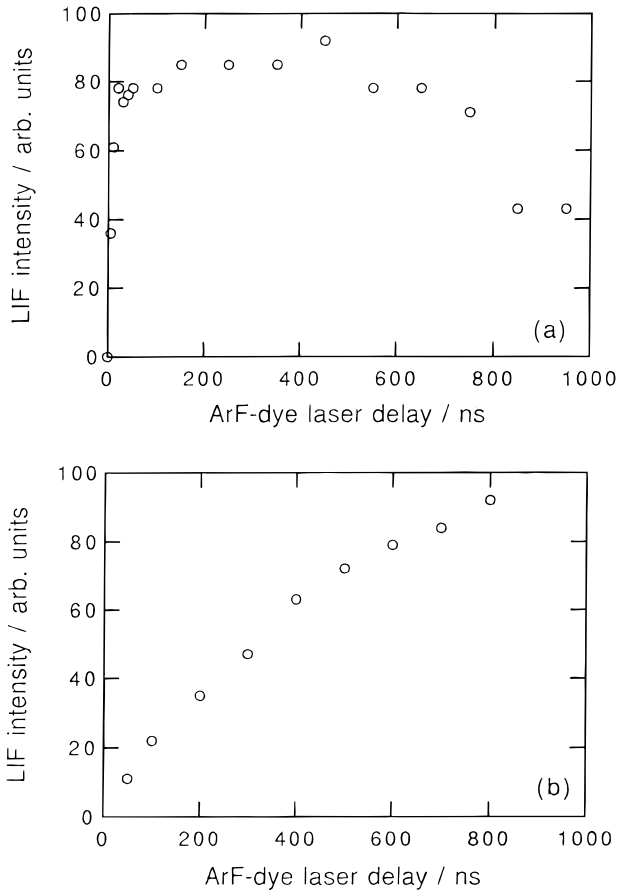

Figure 1. Photolysis probe laser delay dependence of the LIF intensity measured for (a) the reactant-pair reaction and for (b) the bimolecular reaction. In both cases, the Q_{11} (10) lines of ^{16}OH and ^{18}OH are monitored.

were monitored and processed by a boxcar integrator (SRS, SR250). Timing for triggering lasers and the detection system was controlled by a digital delay generator (SRS, DG535).

A premixed gas sample containing 3.93% N_2O in He (Taiyo Sanso) was bubbled through a trap containing $H_2{}^{18}O$ (Eurisotop, 97.1 atom % ^{18}O) whose temperature was controlled with a water−ethylene glycol bath (Komatsu, DW-620, DR-620). It was then expanded through a pulsed nozzle (General Valve, 0.8 mm diam) to produce the $N_2O{\cdot}H_2O$ van der Waals complex. The stagnation pressure was 1.5 atm with 3.93% N_2O and 0.44% $H_2{}^{18}O$ in He. The chamber was pumped by a 6 in. diffusion pump (ANELVA, CDP-1200) equipped with a water-cooled baffle. Typical background pressure in the chamber during the 10 Hz operation of the pulsed nozzle was $(1-2) \times 10^{-4}$ Torr.

III. Results

Prior to the measurement of rotational distributions, several experiments were conducted to ensure that the OH radicals were formed from the $N_2O{\cdot}H_2O$ reactant pair. Figure 1a shows the dependence of the LIF intensity on the photolysis probe laser delay observed at the $Q_{11}(10)$ bands of ^{16}OH and ^{18}OH. The OH signal rises within the laser pulse width and remains constant until ~800 ns, after which it decreases presumably because of the escape of OH from the region of observation. For the sake of comparison, Figure 1b shows a similar result for the bimolecular reaction in a flow cell for a mixture of N_2O (60 mTorr) and $H_2{}^{18}O$ (10 mTorr). In this case, the rise time is much longer than that for the reactant-pair reaction, corresponding to the gas kinetic collision of photoinduced $O(^1D)$ with $H_2{}^{18}O$. The fast rise shown in Figure 1a ensures that the LIF signal is due to the OH formed by the reactant-pair reaction.

Dependence of the LIF intensity on the concentrations of component species was examined at the $Q_{11}(10)$ band. The intensity was found to depend linearly on $[N_2O]$ in the gas mixture before expansion within an error of ±10% in the range $[N_2O] = 0-5\%$. The intensity is also linear with respect to $[H_2O]$ within ±2.7% in the range $[H_2O] = 0-0.5\%$, where $[H_2O]$ is estimated from the vapor pressure of water in the thermostated bath. These results suggest that the OH radicals originate from the 1:1 complex of N_2O and $H_2{}^{18}O$.

The rotational distribution of OH in the $X^2\Pi$ state was determined from the LIF intensity using tabulated values of the Einstein B coefficient,[18] line assignments,[19] and radiative lifetimes of the (v', J') levels in the $A^2\Sigma$ state.[20] Isotopic energy shifts for ^{18}OH were calculated according to the method described in the literature.[8] Common values of the B coefficient were used for ^{16}OH and ^{18}OH.

Boltzmann plots of relative rotational populations determined from the observed LIF spectrum are shown in parts a and b of Figure 2 for $v = 0$ and $v = 1$ of ^{16}OH, respectively, and in Figure 2c for $v = 0$ of ^{18}OH. The rotational distributions fit excellently to the Boltzmann distribution. The Boltzmann temperatures thus determined are summarized in Table 1 together with the previous results for the bimolecular reaction and for the O_3/H_2O system. It should be noted that there is little difference in the rotational temperatures for ^{16}OH and ^{18}OH, in contrast to the corresponding biomolecular reaction.[13] A deviation from the Boltzmann distribution at lower J values in Figure 2c is attributed to ^{18}OH produced by the direct photolysis of uncomplexed $H_2{}^{18}O$ at 193 nm. Although the deviation is observed exclusively for ^{18}OH in the bimolecular reaction,[13] some deviation is observed also for ^{16}OH in the present case (Figure 2a). This is presumably due to the photodissociation of $H_2{}^{18}O$ in the complex, which would produce some ^{16}OH in lower J states.

The relative vibrational population ($v = 1/v = 0$) was obtained by summing up the rotational populations for each vibrational state, where populations for some rotational levels were estimated by extrapolation, since they could not be determined accurately because of band congestion. In contrast to the rotational distribution, the results summarized in Table 1 show a remarkably nonstatistical energy deposition into ^{16}OH and ^{18}OH; newly formed ^{16}OH is vibrationally hot while most of the ^{18}OH stays in the ground vibrational state.

The population ratio in the spin−orbit sublevels was obtained as $F_1N/(F_2(N+1))$, where F_1 and F_2 are the populations in corresponding (degenerate) sublevels and N is the rotational quantum number. It was determined by measuring the Q_{11} and P_{11} transitions for the F_1 ($X^2\Pi_{3/2}$) state and the Q_{22} and P_{22} transitions for the F_2 ($X^2\Pi_{1/2}$) state. The average values of $F_1N/(F_2(N+1))$ are 1.1 ± 0.2, 1.0 ± 0.2, and 1.2 ± 0.2 for ^{16}OH $v'' = 0$ and $v'' = 1$ and for ^{18}OH $v'' = 0$, respectively, showing no propensity for one of the sublevels.

The population ratio for the Λ-doublet components, $\lambda \equiv A'/A''$, was determined using the P and Q transitions. The λ value was found to depend little on J, giving the average value of λ to be 1.1 ± 0.2, 1.2 ± 0.3, and 1.3 ± 0.2 for ^{16}OH $v'' = 0$ and $v'' = 1$ and for ^{18}OH $v'' = 0$, respectively; namely, there is little propensity for A' or A''.

The rotational energy for ^{16}OH or ^{18}OH can be obtained as

$$E_R(v) = R_g T_R(v) \qquad (2)$$

where R_g is the gas constant and $T_R(v)$ is the rotational temperature for the vth vibrational state. The average vibrational

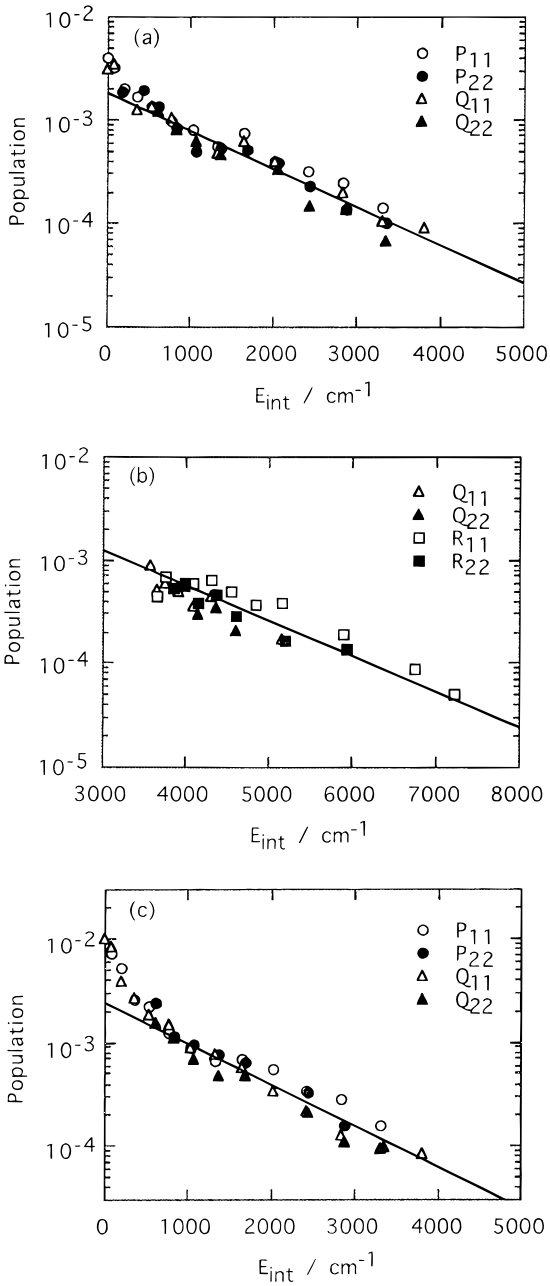

Figure 2. Relative populations in rotational levels of OH (divided by degeneracy $2J + 1$) plotted against the internal energy $E_{int} = E_R + E_V$: (a) $v = 0$ and (b) $v = 1$ of ^{16}OH; (c) $v = 0$ of ^{18}OH. Symbols denote the rotational branches as P_{11} (○), P_{22} (●), Q_{11} (△), Q_{22} (▲), R_{11} (□), and R_{22} (■).

energy for ^{16}OH or ^{18}OH is given by

$$E_R = \sum_V \rho(v)E_R(v)/\sum_V \rho(v) \quad (3)$$

where $\rho(v)$ is the relative vibrational population and the summation is taken over vibrational states. The average energy in the vibrational degrees of freedom for ^{16}OH or ^{18}OH is given by

$$E_V = \sum_V \rho(v)E_V(v)/\sum_V \rho(v) \quad (4)$$

where $E_V(v)$ is the vibrational energy above $v = 0$: $E_V(1) = 42.7$ kJ mol^{-1} for ^{16}OH and $E_V(1) = 42.5$ kJ mol^{-1} for ^{18}OH.[21,22] $E_R(v)$, $E_V(v)$, E_R, and E_V for ^{16}OH and ^{18}OH calculated by means of (2)−(4) are summarized in Table 2. For the sake of comparison, corresponding data for the bimolecular reaction and the reactant-pair and bimolecular reactions in the O_3/H_2O systems are included in the table.

TABLE 1: Observed Rotational Temperatures (T_R) and Relative Vibrational Populations of ^{16}OH and ^{18}OH Produced in the Reactant-Pair and Bimolecular Reactions

	$N_2O/H_2{}^{18}O$		$O_3/H_2{}^{18}O$	
	reactant pair	bimolecular[a]	reactant pair[b]	bimolecular[c]
		^{16}OH		
$T_R(v = 0)$/K	1700	6000	1300	4900
$T_R(v = 1)$/K	1700	2200	1300	4000
ρ_1/ρ_0[d]	0.41	0.68	0.23	0.74
		^{18}OH		
$T_R(v = 0)$/K	1600	2600	1100	2700
$T_R(v = 1)$/K		2200		2300
ρ_1/ρ_0[d]	0	0.04	<0.04	0.06

[a] Reference 13. [b] Reference 14. [c] Reference 11. [d] ρ_1 and ρ_0 are the populations in the $v = 1$ and $v = 0$ states, respectively.

TABLE 2: Summary of the Rotational and Vibrational Energies (kJ mol^{-1})

	$N_2O/H_2{}^{18}O$		$O_3/H_2{}^{18}O$	
	reactant pair	bimolecular[a]	reactant pair[b]	bimolecular[c]
		^{16}OH		
$E_R(v = 0)$	14.1	49.9	10.8	40.7
$E_R(v = 1)$	14.1	18.3	10.8	33.3
$E_R(^{16}OH)$[d]	14.1	37.1	10.8	37.6
		^{18}OH		
$E_R(v = 0)$	13.3	21.6	9.15	22.4
$E_R(v = 1)$		18.3		19.1
$E_R(^{18}OH)$[d]	13.3	21.5	9.15	22.3
E_R[e]	27.4	58.6	20.0	59.9
$\Delta E/E_R$[f]	0.0292	0.27	0.0825	0.26
$E_V(^{16}OH)$[g]	12.4	17.3	7.98	18.2
$E_V(^{18}OH)$[g]	0	1.6	1.6	2.6
E_V[h]	12.4	18.9	9.58	20.8
E_{avail}[i]	387	165.1	280	142.0
$E_i(^{16}OH)/E_{avail}$[j]	0.0685	0.329	0.0671	0.393
$E_i(^{18}OH)/E_{avail}$[j]	0.0344	0.140	0.0384	0.175
E_R/E_{avail}	0.0708	0.35	0.0714	0.48
E_V/E_{avail}	0.0320	0.11	0.0342	0.15

[a] Reference 13. [b] Reference 14. [c] Reference 11. [d] Calculated with eq $E_R(OH) = \sum_V \rho(v)E_R(v)/\sum_V \rho(v)$. [e] $E_R = E_R(^{16}OH) + E_R(^{18}OH)$. [f] $\Delta E = E_R(^{16}OH) - E_R(^{18}OH)$. [g] Calculated with eq $E_V(OH) = \sum_V \rho(v)E_V(v)/\sum_V \rho(v)$. [h] $E_V = E_V(^{16}OH) + E_V(^{18}OH)$. [i] See text. [j] $E_i(^{16}OH) = E_R(^{16}OH) + E_V(^{16}OH)$, $E_i(^{18}OH) = E_R(^{18}OH) + E_V(^{18}OH)$.

IV. Discussion

A. Energetics. Energy levels for the species related to the 193 nm photolysis of the $N_2O{\cdot}H_2O$ complex are presented schematically in Figure 3, where the stabilization energy due to the complex formation is ignored. Energies measured from the ground state of the complex are shown for each level, which have been calculated from known values of heats of formation.[23] Those in parentheses have been estimated by ab initio calculations.[24,25] The figure shows that the 193 nm photolysis of the complex into $N_2 + 2OH$ leaves $619 - 232 = 387$ kJ mol^{-1} of excess energy to be partitioned among the internal and translational degrees of freedom of products.

Three possible intermediates are shown in the figure, one of which is hydrogen peroxide known to be stable in its ground state. Actually, the photolysis of $O_3{\cdot}H_2O$ in the argon matrix gave H_2O_2 as a product.[26] However, in the present case, where the excess energy is not dissipated, H_2O_2 is not stabilized and the system goes to the final state. The first singlet excited state (^{1}A) of H_2O_2 lies slightly higher than 619 kJ mol^{-1} [27] corre-

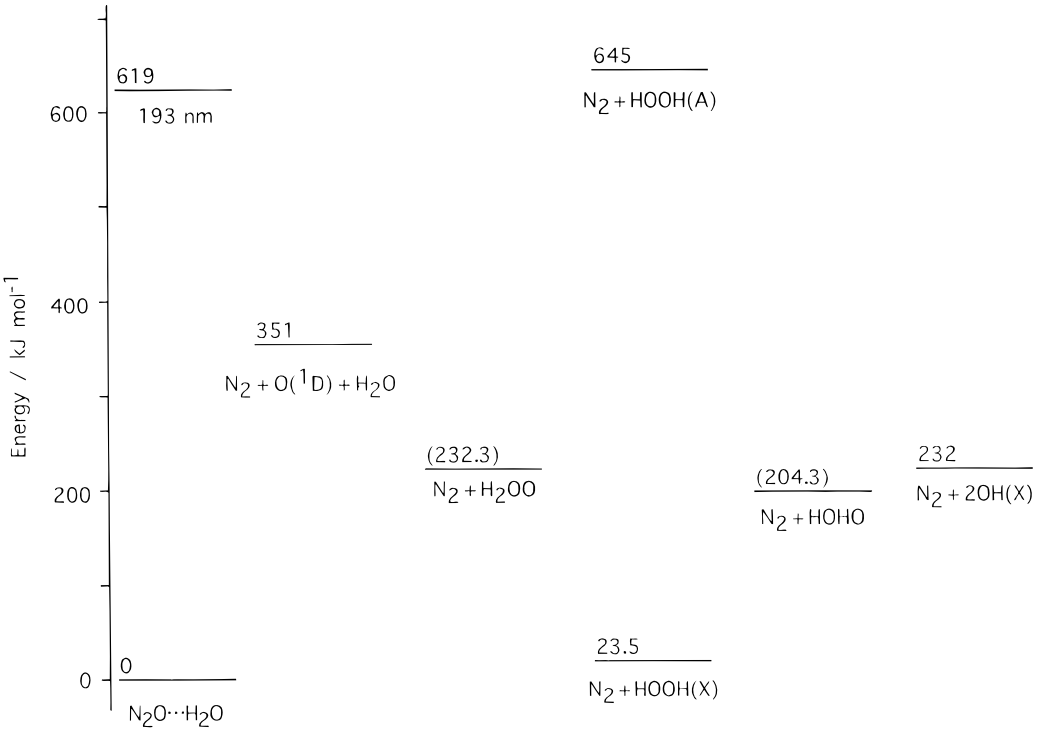

Figure 3. Energy level diagram for the reaction $N_2O{\cdot}H_2{}^{18}O + h\nu \rightarrow N_2 + {}^{16}OH + {}^{18}OH$. Number on each level represents the energy (kJ mol^{-1}) from the ground state of $N_2O{\cdot}H_2{}^{18}O$. See text for the source of these values.

sponding to the 193 nm excitation and cannot be accessed by the photolysis of the complex. However, in the distorted form of H_2O_2, it may come down considerably[28] and would play a role by interacting with other surfaces.

An ab initio calculation on the $OH + OH \rightarrow H_2O + O(^1D)$ reaction has shown the formation of a hydrogen-bonded complex OH···OH as an intermediate.[24] The transition states leading to the formation of H_2O and $O(^1D)$ from OH···OH were calculated to be 8.8 kJ mol^{-1} above $O(^1D) + H_2O$.

The 1,2-hydrogen shift of hydrogen peroxide is known to give water oxide, H_2OO.[25,29] An ab initio calculation has predicted the ground state of H_2OO to lie at 195 kJ mol^{-1} above the ground state of H_2O_2 with an activation energy of 229 kJ mol^{-1}, while the reverse reaction, $H_2O_2 \rightarrow H_2OO$, has a lower barrier of 33.9 kJ mol^{-1}.[25] As shown in Figure 3, it lies very close to the final state, $N_2 + 2OH$, and its surface has correlations with $O(^1D) + H_2O$ and with H_2O_2.

B. Conformation of the Complex and Excited-State Geometry. Conformation of the $N_2O{\cdot}H_2O$ complex has been determined experimentally.[30] Since the result has large ambiguity, we have performed an ab initio calculation on the ground state of $N_2O{\cdot}H_2O$ by optimizing all bond distances and angles using MP4(SDTQ)/6-311G** with Gaussian 92. The result is illustrated in Figure 4, where the covalent bond radii are indicated by shaded circles. The distance 2.08 Å between one of the hydrogens and O in N_2O corresponds to the sum of the van der Waals bond radii, indicating that complex formation is exclusively due to the van der Waals force and not to hydrogen bonding as expected. The figure shows that the O−H···O bond is linear but the H···ON bond angle is 124°. Therefore, for an efficient reaction to occur, the dissociated O atom is required to have a considerable velocity component perpendicular to the N−N−O axis.

The electronic absorption band of N_2O in the 193 nm region is part of a weak continuum that originated from the $^1\Delta \leftarrow {}^1\Sigma^+$ and $^1\Sigma^- \leftarrow {}^1\Sigma^+$ transitions.[31] Both are forbidden in the linear configuration but become allowed in a bent structure. The $^1\Delta$ state splits into a Renner−Teller pair, $2^1A'$ ($B^1\Delta$) and $2^1A''$

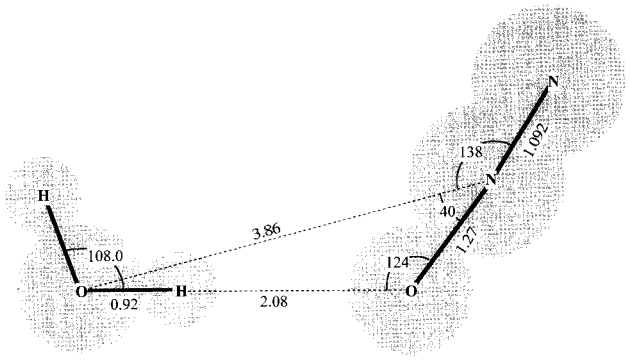

Figure 4. Structure of the $N_2O{\cdot}H_2O$ complex obtained by an ab initio calculation. Bond distances and angles are given in units of angström and degree, respectively. The shaded circles represent the covalent bond radius.

($B^1\Delta$), in the bent geometry. Hanisco and Kummel investigated the photodissociation of N_2O at 203−205 nm using REMPI (resonance-enhanced multiphoton ionization),[32] confirming that the vibronically allowed parallel transition ($A' \leftarrow A'$) to the $2^1A'$ ($B^1\Delta$) state in the bent excited state is responsible for the photodissociation. Unusually high rotational excitation of N_2 has been reported for the 193 nm photodissociation of N_2O.[33,34] This result could only be accounted for by assuming a strong kick-out of $O(^1D)$ sideways with respect to the molecular axis. Qualitatively the same argument would apply to photodissociation in the complex; namely, the oxygen atom is kicked out sideways, which is favored to interact with H_2O in view of the conformation in Figure 4. It should be noted that the calculated planar conformation is the lowest-energy one. Since the weak van der Waals interaction gives rise to only very low barriers to the mutual rotational motion of H_2O and N_2O in the complex, we should have observed an average of several mutual orientations of H_2O and N_2O even under the supersonic cooling.

C. Dynamics. Table 2 shows that $E_R({}^{16}OH)$ and $E_R({}^{18}OH)$ are nearly the same in the reactant-pair reaction of $N_2O{\cdot}H_2O$. This is in sharp contrast with the corresponding bimolecular

reaction, where the large difference between $E_R(^{16}OH)$ and $E_R(^{18}OH)$ has been attributed to spectator-stripping mechanism.[13] The situation is qualitatively the same for the O_3/H_2O system, although the absolute values of energy is different because of the difference of the excess energies.

It is to be emphasized that the ratios of the total rotational and vibrational energies to the available energy, E_R/E_{avail} and E_V/E_{avail}, and of the internal energies for ^{16}OH and ^{18}OH to the available energy, $E_i(^{16}OH)/E_{avail}$ and $E_i(^{18}OH)/E_{avail}$, are almost the same for $N_2O{\cdot}H_2O$ and $O_3{\cdot}H_2O$ despite the difference in their E_{avail} and conformations.[14] This fact seems to suggest strongly that both reactant-pair reactions proceed through a common intermediate, $[O{\cdot}H_2O]$. In other words, the restriction of relative orientation or collision cross section due to complex formation is not the primary factor governing the dynamics. Rather, it should be stressed that the primary effect of complex formation is to control the "collision" of the dissociated O atom with H_2O so that a "soft" collision occurs to form an intermediate and to remove much of the excess energy as translational and internal energies of the counterpart (N_2 or O_2). This is in contrast to the bimolecular reactions, where the "hard" collision gives more energy to the internal degrees of freedom of OH in a nonstatistical manner.

In view of the above-mentioned considerations, we may consider the following reaction scheme:

$$N_2O{\cdot}H_2{}^{18}O + h\nu \rightarrow [N_2{\cdot}OH_2{}^{18}O] \quad (5)$$

$$\rightarrow N_2 + [O{\cdot}H_2{}^{18}O] \quad (6)$$

$$\rightarrow N_2 + (H_2O_2) \quad (7)$$

$$\rightarrow N_2 + {}^{16}OH + {}^{18}OH \quad (8)$$

where $[O{\cdot}H_2{}^{18}O]$ is a hypothetical "initial" state of the intermediate right after the departure of N_2, while (H_2O_2) is a metastable intermediate ($HO^{18}OH$, $OH^{18}OH$, or $H_2{}^{18}OO$). Among them, $OH^{18}OH$ and $H_2{}^{18}OO$ have direct correlations with the initial state $[O{\cdot}H_2{}^{18}O]$ while $HO^{18}OH$ does not. On the other hand, $HO^{18}OH$ and $OH^{18}OH$ are directly correlated with the final state ($^{16}OH + {}^{18}OH$) while $H_2{}^{18}OO$ is not.

Table 2 shows that E_R is almost even for ^{16}OH and ^{18}OH, while there is a remarkable difference in E_V. This means that the excess energy is not randomized completely in the intermediate. This may be consistent with the observation of the rise time of OH signal (Figure 1), indicating the lifetime of the intermediate to be shorter than 10 ns. However, it is difficult to accept the idea that, in a certain lifetime of the intermediate, the rotational energy is randomized completely while the vibrational energy is strongly localized. It should therefore be understood that the energy partition is due to dynamical processes such as (5)−(8) rather than to the randomization process.

Among several possible channels involving the intermediate, the formation of two OH's through HOOH may be rejected, since it is difficult to consider the vibrational energy to be localized in one of the equivalent OH bonds. On the other hand, the formation of ^{16}OH and ^{18}OH from $OH^{18}OH$ could account for it; namely, if its conformation is such that ^{16}O lies on the extension of one of the H−O bonds in $H_2{}^{18}O$ and if the transfer of H from ^{18}O to ^{16}O occurs on the potential surface with an early barrier, the resultant ^{16}OH should be vibrationally highly excited while ^{18}OH should not. The even rotational energies in ^{16}OH and ^{18}OH may be understood as follows. During the dissociation of $OH^{18}OH$, the torque operated through the $^{16}O\cdots H-{}^{18}O$ bond is directed toward the ^{16}O atom, giving little rotational motion to ^{16}OH. The torque is also operated on $^{18}O-H$, but the center of gravity of $^{18}O-H$ is very close to the center of the O atom, resulting in a very weak rotational excitation of ^{18}OH. Most of the rotational excitation may result from the transfer of overall rotational motion of $OH^{18}OH$. The latter is given when N_2 departs the system. If the conformation of the complex is as shown in Figure 4, the resultant rotational excitation after bond breaking should be confined in the molecular plane of $OH^{18}OH$. However, the highly flexible structure of the van der Waals complex could allow the oxygen atom to attack H_2O in various relative orientations, giving nearly even rotational excitation around three axes of rotation of $OH^{18}OH$. This, combined with the flexibility in the conformation of $OH^{18}OH$ itself, would result in the even rotational distribution over ^{16}OH and ^{18}OH. This scheme would also account for the nearly statistical distribution observed for the Λ-doublets.

To obtain further insight on the dissociation scheme, we have applied a generalized impulsive model[35] to the present case. This model assumes that atoms α and β in fragments A and B, respectively, in the parent molecule A−B form a bond and, upon dissociation, α and β receive the translational energy while the remaining parts of A and B are fixed. Atom α is assumed to undergo a completely inelastic collision with the rest of A. If we assume the linear momentum conservation, translational energy is not conserved. The difference of energy is assumed to be used for internal excitation of A. The same holds for fragment B. The model predicts, therefore, the higher limit of internal excitation of fragments. In the case of OHOH formation from the complex, this model predicts 111 and 111 kJ mol^{-1}, out of $E_{avail} = 619 - 204.3 = 415$ kJ mol^{-1} (see Figure 3), partitioned into the translational and internal energies of N_2, respectively, while OHOH receives 86 and 108 kJ mol^{-1} as translational and internal energy, respectively. In the case of H_2OO formation from the complex, N_2 receives 103 and 103 kJ mol^{-1}, out of $E_{avail} = 619 - 232.3 = 387$ kJ mol^{-1} (see Figure 3), as the translational and internal energies, respectively, while H_2OO receives 80 and 100 kJ mol^{-1} in translational and internal energy, respectively. The energy partitioned into N_2 is almost the same or less than that of 220 kJ mol^{-1} measured in the photolysis of N_2O at 193 nm.[33,34]

Now let us try to apply the same impulsive model to the dissociation of $OH^{18}OH$ and HOOH. For the latter, we assume that HOOH is formed through H_2OO and dissociates into 2OH. The above estimation gave the internal energy of 100 kJ mol^{-1} for H_2OO. Considering the energy difference between H_2OO and 2OH (Figure 3), the available energy to be partitioned is $E'_{avail} = 100 + 232.3 - 232 = 100$ kJ mol^{-1}. The impulsive model calculation for $HO^{18}OH$ gives the internal energies as $E_i(^{16}OH) = 3.1$ kJ mol^{-1} and $E_i(^{18}OH) = 2.5$ kJ mol^{-1}. They correspond to 0.8% and 0.6%, respectively, of the total available energy of 387 kJ mol^{-1}, which should be compared with the observation of 6.9% and 3.4%, respectively (Table 2). Since the present model gives the higher limit for the internal energy, the model cannot account for the observed internal excitation.

The internal energy for $OH^{18}OH$ is 108 kJ mol^{-1} as obtained above. Considering the energy difference between $OH^{18}OH$ and 2OH, $E''_{avail} = 108 + 204.3 - 232 = 80$ kJ mol^{-1}, which is partitioned into the internal degrees of freedom as $E_i(^{16}OH) = 71$ kJ mol^{-1} and $E_i(^{18}OH) = 0.2$ kJ mol^{-1}, corresponding to 18% and 0.05%, respectively, of the total available energy, 387 kJ mol^{-1}. This accounts for the observed trend qualitatively, although the deviation from the even distribution is exaggerated in the calculation. It is presumably due to the rigid conformation

of $OH^{18}OH$ assumed in the calculation; the energy partition would approach the observed one if the flexibility of ^{16}O around the $^{16}O\cdots H-{}^{18}O$ axis is taken into account. Thus, the crude estimation based on the impulsive model also supports the role of $OH^{18}OH$ as an intermediate.

V. Conclusion

We have determined the vibrational and rotational distributions in ^{16}OH and ^{18}OH produced by the 193 nm photodissociation of the van der Waals complex, $N_2O\cdot H_2{}^{18}O$. The result shows almost even rotational distribution in ^{16}OH and ^{18}OH in sharp contrast to the corresponding bimolecular reaction, while the vibrational excitation is localized in ^{16}OH. This tendency is qualitatively the same as that observed previously for the O_3/H_2O system. The extreme similarity of the mode of energy partitioning between the $N_2O\cdot H_2O$ and $O_3\cdot H_2O$ systems has led us to conclude that the energy partitioning is predominantly determined by the dynamical process in the short-lived intermediate formed after the departure of N_2 (or O_2) from the system. These considerations, together with the calculated molecular structure of the complex, have led us to propose an intermediate of the type of $OH^{18}OH$ responsible for the observed internal energy distribution. Naturally, more experimental evidence is required before this hypothesis is fully rationalized. In particular, experimental determination of the translational energy distributions for N_2, ^{16}OH, and ^{18}OH would be helpful. This is in progress in our laboratory.

Acknowledgment. This work was partly defrayed by the Grant-in-Aid on Priority-Area-Research on "Photoreaction Dynamics" from the Ministry of Education, Science, Sports, and Culture of Japan (06239103). We are grateful for the use of an excimer laser (Lambda Physik, COMPex 200) of the Instrument Center of IMS.

References and Notes

(1) Buelow, S.; Radhakrishnan, G.; Catanzarite, J.; Wittig, C. *J. Chem. Phys.* **1985**, *83*, 444.

(2) Honma, K.; Kajimoto, O. *Chem. Phys. Lett.* **1985**, *117*, 123.

(3) Sivakumar, N.; Burak, I.; Cheung, W.-K.; Houston, P. L.; Hepbern, J. W. *J. Phys. Chem.* **1985**, *89*, 3609.

(4) For example: Takayanagi, M.; Hanazaki, I. *Chem. Rev.* **1991**, *91*, 1193. Shin, S. K.; Chen, Y.; Nickolaisen, S.; Sharpe, S. W.; Beaudet, R. A.; Wittig, C. *Adv. Photochem.* **1991**, *16*, 249. Fujimura, Y. *J. Spectrosc. Soc. Jpn.* **1993**, *42*, 349.

(5) Gericke, K. H.; Ortgies, G.; Comes, F. J. *Chem. Phys. Lett.* **1980**, *69*, 156.

(6) Gericke, K.; Comes, F. J. *Chem. Phys. Lett.* **1980**, *74*, 63.

(7) Comes, F. J.; Gericke, K.; Manz, J. *J. Chem. Phys.* **1981**, *75*, 2853.

(8) Butler, J. E.; Talley, L. D.; Smith, G. K.; Lin, M. C. *J. Chem. Phys.* **1981**, *74*, 4501.

(9) Gericke, K.; Comes, F. J.; Levine, R. D. *J. Chem. Phys.* **1981**, *74*, 6106.

(10) Cleveland, C. B.; Wiesenfeld, J. R. *J. Chem. Phys.* **1992**, *96*, 248.

(11) Sauder, D. G.; Stephenson, J. C.; King, D. S.; Casassa, M. P. *J. Chem. Phys.* **1992**, *97*, 952.

(12) King, D. S.; Sauder, D. G.; Casassa, M. P. *J. Chem. Phys.* **1992**, *97*, 5919.

(13) Tanaka, N.; Takayanagi, M.; Hanazaki, I. *Chem. Phys. Lett.* **1996**, *254*, 40.

(14) King, D. S.; Sauder, D. G.; Casassa, M. P. *J. Chem. Phys.* **1994**, *100*, 4200.

(15) Kim, H. L.; Takayanagi, M.; Hanazaki, I. *Chem. Phys. Lett.* **1994**, *222*, 431.

(16) Paraskevopoulos, G.; Cvetanovic, R. J. *J. Am. Chem. Soc.* **1969**, *91*, 7572.

(17) Sparks, R. K.; Carlson, L. R.; Shobatake, K.; Kowalczyk, M. L.; Lee, Y. T. *J. Chem. Phys.* **1980**, *72*, 1401.

(18) Chidsey, I. L.; Crosley, D. R. *J. Quant. Spectrosc. Radiat. Transfer* **1980**, *23*, 187.

(19) Dieke, G. H.; Crosswhite, H. M. *J. Quant. Spectrosc. Radiat. Transfer* **1962**, *2*, 97.

(20) Brzozowski, J.; Erman, P.; Lyyra, M. *Phys. Scr.* **1978**, *17*, 507.

(21) Huber, K. P.; Herzberg, G. *Molecular Spectra and Molecular Structure IV. Constants of Diatomic Molecules*; Van Nostrand: New York, 1979.

(22) Maillard, J. P.; Chauville, J. *J. Mol. Spectrosc.* **1976**, *63*, 120.

(23) Chase, N. W., Jr.; Davies, C. A.; Downey, J. R., Jr.; Frurip, D. J.; McDonald, R. A.; Syverud, A. N. *J. Phys. Chem. Ref. Data Suppl. 1* **1985**, *14*.

(24) Fueno, T. *Applied Quantum Chemistry*; Smith, V. H., Schaefer, H. F. Morokuma, K., Eds.; Reidel: Dordrecht, 1986; p 33.

(25) Hrusak, J.; Friedrichs, H.; Schwarz, H.; Razafinjanahary, H.; Chermette, H. *J. Phys. Chem.* **1996**, *100*, 100.

(26) Schriver, L.; Barreau, C.; Schriver, A. *Chem. Phys.* **1990**, *140*, 429.

(27) Chevaldonnet, C.; Cardy, H.; Dargelos, A. *Chem. Phys. Lett.* **1986**, *102*, 55.

(28) Gericke, K.; Klee, S.; Comes, F. J.; Dixon, R. N. *J. Chem. Phys.* **1986**, *85*, 4463.

(29) Meredith, C.; Hamilton, T. P.; Schaefer, H. F., III. *J. Phys. Chem.* **1992**, *96*, 9250.

(30) Zolandz, D.; Yaron, D.; Peterson, K. I.; Klemperer, W. *J. Chem. Phys.* **1992**, *97*, 2861.

(31) Rabalais, J. W.; McDonald, J. M.; Scherr, V.; McGlynn, S. P. *Chem. Rev.* **1971**, *71*, 73.

(32) Hanisco, T. F.; Kummel, A. C. *J. Phys. Chem.* **1993**, *97*, 7242.

(33) Felder, P.; Haas, B.; Huber, J. R. *Chem. Phys. Lett.* **1991**, *186*, 177.

(34) Springsteen, L. L.; Satyapal, S.; Matsumi, Y.; Dobeck, L. M.; Houston, P. L. *J. Phys. Chem.* **1993**, *97*, 7239.

(35) Trentelman, K. A.; Kable, S. H.; Moss, D. B.; Houston, P. L. *J. Chem. Phys.* **1989**, *91*, 7498.